Simulations of Binary Black Hole Mergers

Dale Choi

KISTI Supercomputing Center, KISTI, Daejeon, Korea & NASA/GSFC

Supported by The Korea Research Foundation and The Korean Federation of Science and Technology Socities Grant funded by Korea Government (MOEHRD, Basic Research Promotion Fund)

Simulations supported by Project Columbia (NASA Ames Research Center) and NASA Center for Computational Sciences (NASA/GSFC)

Department of Physics, Hanyang University, Seoul, Korea, NOV 24, 2006

Outline

- Gravitational Wave (Astro)Physics
- Numerical Relativity
- Simulations of Binary Black Hole Mergers

- Collaborators: J. Centrella, J. Baker, J. van Meter, B. Kelly, D. Boggs (NASA/GSFC), M. Koppitz (AEI), M. C. Miller (UMD), and G.-W. Kang & S.-M. Lee (KISTI)

Introduction

- Among the key predictions of Einstein's general theory of relativity are black holes and gravitational waves.
- Gravitational waves (GWs) are weak-field (linearized) solutions that represent the freely propagating degrees of freedom of the gravitational field.
- GWs are produced in the physical scenarios such as merger of two black holes, or supernovae explosions.
- As early as 1917, Einstein recognized their existence.
- There exists indirect evidence for GW from Hulse-Taylor pulsar, PSR 1913+16: observed change in the period of the binary orbit matches well with the predictions from GR within 1%.
- But, in November 2006, gravitational waves have yet to be directly detected.

Gravitational Waves

Gravitational waves are fundamentally different from electromagnetic radiations:

- Warpage of spacetime itself (cf. E&M: oscillations of E&M fields propagate through the background spacetime).
- Produced by coherent superpositions of radiation due to the bulk dynamics of the source (cf. E&M: incoherent superposition of excitations of individual particles).
- Interact very weakly with matter (cf. E&M interact strongly with matter).
- Thus provide direct information about the system's dynamics. (cf. E&M: direction information about the thermodynamic state).
- Wavelength of GWs typically of order or larger than the size of the source (cf. E&M: wavelength typically smaller than the radiating system).

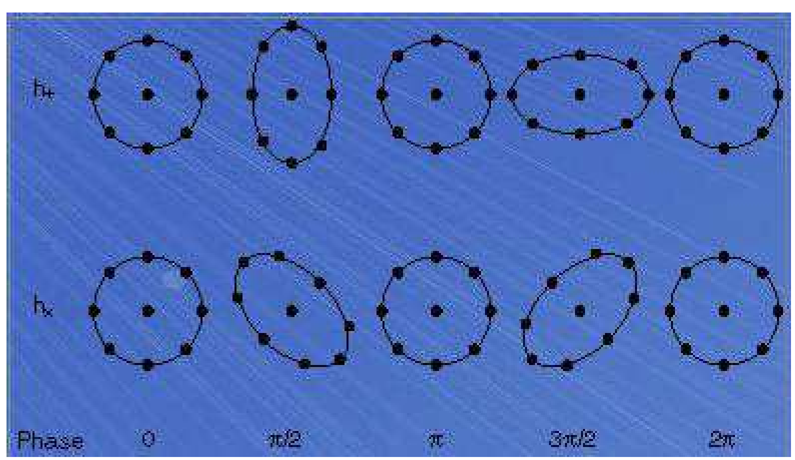

GW Detection

- Roughly speaking, distance travelled by laser beams between the test masses change when gravitational waves pass through. Detectors will measure strain amplitude, $h = \frac{\Delta L}{L}$.

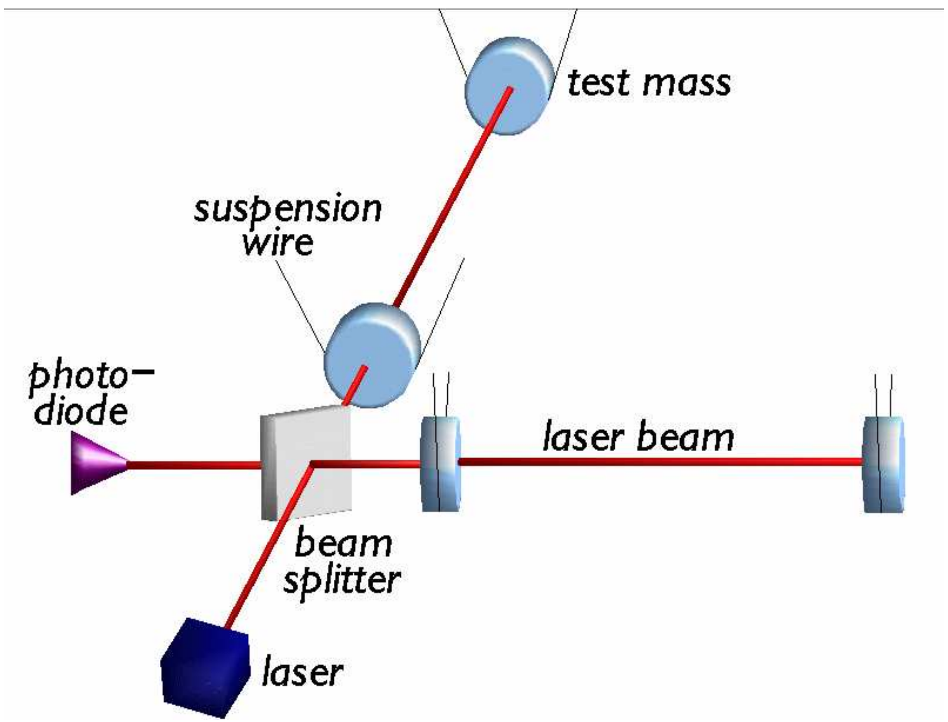

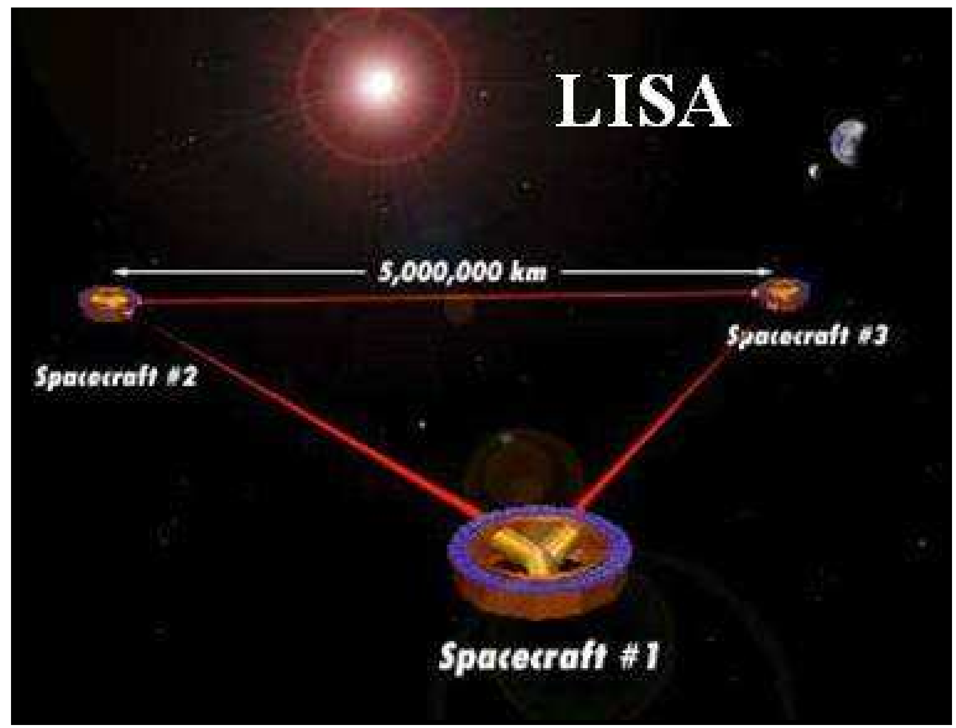

GW Detection

- For typical sources for LIGO, $h = \frac{\Delta L}{L} = 10^{-21} - 10^{-22}$ or smaller.
- Size of Earth $R_{earth} \sim 10^7 m$, Size of atomic nucleus $R_{nulc} \sim 10^{-15} m$. $h \sim \frac{R_{nulc}}{R_{earth}}$!!
- A passing GWs will perturb arm lengths leading to a phase shift in the laser pulse that will disturb interference pattern.
- If the laser beams bounce back-and-forth 100 times within the cavities, the accumulated phase shifts would be $\delta\phi \sim 2 \times 100 \frac{2\pi}{\lambda} \delta L$, where λ is laser wavelength.

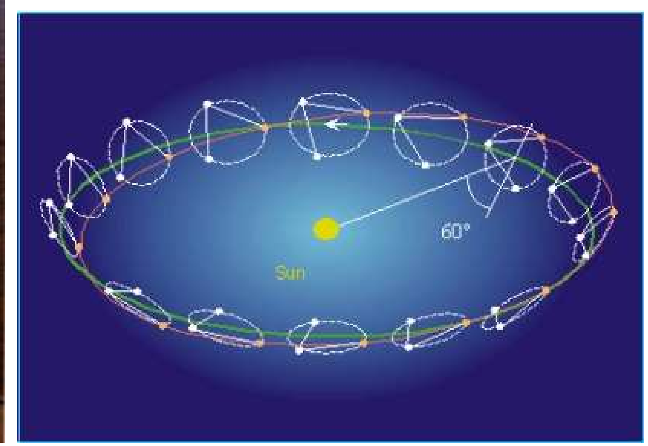

GW Sources

- Requires the systems with the strong time-dependent quadrupole moments.
- Coalescing compact binary systems are the best understood sources of GWs.
- Stellar mass (Super-Massive) black hole binaries are among the main source of GWs for LIGO (LISA) gravtiational wave observatories.
- Ultimate goal of Gravitational Wave Astronomy is to use GW as a tool to study astrophysics and fundamental physics.
- GWs can come from the sources deeply embedded in the centers of the galaxies and regions and carry information about the spacetime geometry in the region of the extremely strong gravity.
- GWs will open a new window into the universe!

Supermassive Binary Black Holes

- Super-Massive BHs (with $\sim 10^5 - 10^9 M_{sun}$) are believed to be central engines of the most active galatic nuclei and play major roles in formation and evolution of galaxies and various dynamical phenomena such as jets.
- Following a galactic merger, a binary black hole system will be formed that can eventaully merge into a single black hole emitting gravitational waves.

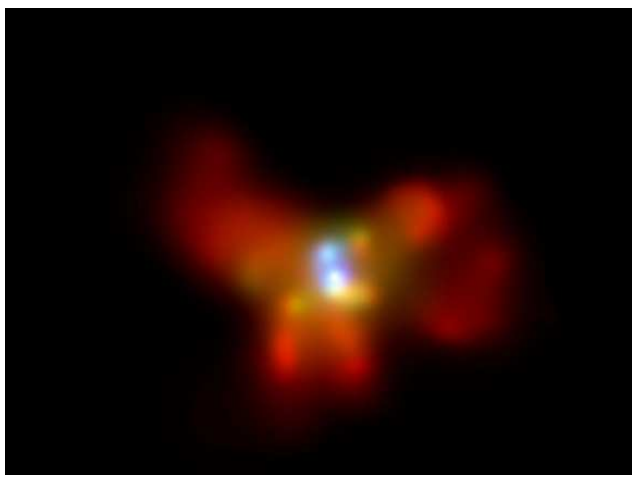
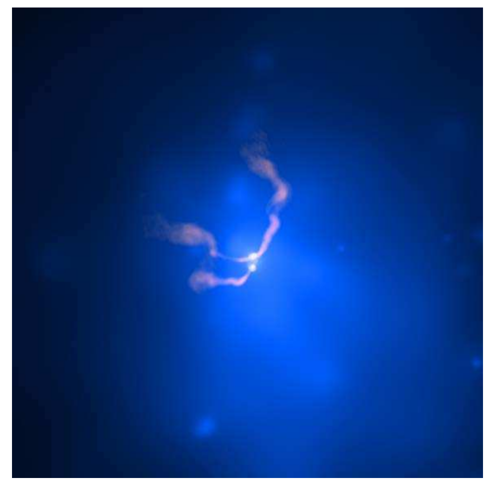

Left (NGC 6240 X-ray image), Right (X-ray(blue) and Radio (pink) images of Abell 400 galaxy cluster)

- Detection and parameter extraction of mergers will be greatly improved by the theoretical templates of the waveforms.

Numerical Relativity

- The complex nature of the merger problem necessitate a computational approach $\rightarrow$ Numerical Relativity.
- We use large high performance computers to simulate various physical processes in black hole interactions and then attempt to extract the salient physics from the results of the simulations.
- Basic idea is to formulate Einstein field equations so as to pose initial(-boundary) value problems for the spacetime geometry.
- Most popular approach is “3+1” where 4D spacetime is foliated by the spacelike (3D) hypersurface.

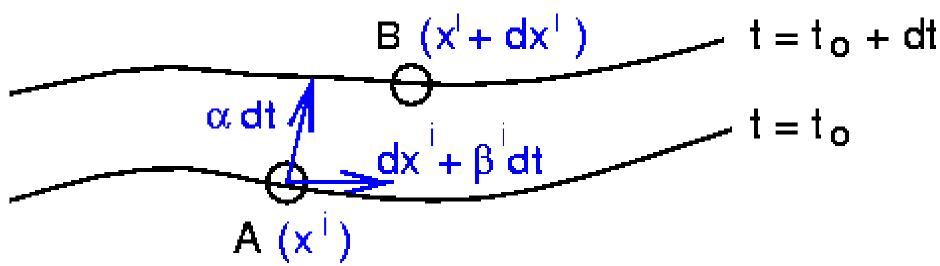

Numerical Relativity

- Einstein Equations in "3+1" approaches are broken into two kinds: constraint equations and evolution equations.
- Constraint equations:

$$R + K^2 - K_{ij}K^{ij} = 0$$
$$D_j K_i^j - D_i K = 0$$

- Evolutions equations (next slide).
- Adopt free evolution: constraint equations are solved only at the initial time, and solutions are constructed by evovling the initial data by evolution equations (only).
- Constraint equations are guaranteed to be satisfied via Bianchi identities at the continuum level. For numerical simulations, constraint equations are only monitored for $t > 0$.

Methods

- $ds^2 = -\alpha^2 dt^2 + \gamma_{ij}(dx^i + \beta^i dt)(dx^j + \beta^j dt)$
- A version of BSSN system of equations with variables $\{\tilde{\gamma}_{ij}, \phi, \tilde{A}_{ij}, K, \tilde{\Gamma}^i\}$ defined from the usual ADM variables $\{\gamma_{ij}, K_{ij}\}$.

$$\begin{aligned}
\phi &= \frac{1}{12}\log\gamma \\
K &= \gamma^{ab}K_{ab} \\
\tilde{\gamma}_{ij} &= e^{-4\phi}\gamma_{ij} \\
\tilde{A}_{ij} &= e^{-4\phi}\left(K_{ij} - \frac{1}{3}\gamma_{ij}K\right) \\
\tilde{\Gamma}^i &= \tilde{\gamma}^{ab}\tilde{\Gamma}^i_{ab}
\end{aligned}$$

where $\tilde{\Gamma}^i_{ab}$ Christoffel symbol associated with the conformal metric $\tilde{\gamma}_{ij}$.

- $\{\tilde{\gamma}_{ij} \equiv \tilde{\gamma}_{ij}(t,x,y,z), \phi \equiv \phi(t,x,y,z), \tilde{A}_{ij} \equiv \tilde{A}_{ij}(t,x,y,z), K \equiv K(t,x,y,z), \tilde{\Gamma}^i \equiv \tilde{\Gamma}^i(t,x,y,z)\}$

Methods

- Equation of motion for $\{\tilde{\gamma}_{ij}, \phi, \tilde{A}_{ij}, K, \tilde{\Gamma}^i\}$

$$
\begin{aligned}
\frac{d\phi}{dt} &= -\frac{1}{6}\alpha K \\
\frac{dK}{dt} &= -\nabla^a\nabla_a\alpha + \alpha\left(\tilde{A}_{ab}\tilde{A}^{ab} + \frac{1}{3}K^2\right) \\
\frac{d\tilde{\gamma}_{ij}}{dt} &= -2\alpha\tilde{A}_{ij} \\
\frac{d\tilde{A}_{ij}}{dt} &= e^{-4\phi}\left(-\nabla_i\nabla_j\alpha + \alpha R_{ij}\right)^{\mathrm{TF}} + \alpha\left(K\tilde{A}_{ij} - 2\tilde{A}_{ia}\tilde{A}^a{}_j\right) \\
\frac{\partial\tilde{\Gamma}^i}{\partial t} &= 2\alpha\left(\tilde{\Gamma}^i_{ab}\tilde{A}^{ab} - \frac{2}{3}\tilde{\gamma}^{ia}K_{,a} + 6\tilde{A}^{ia}\phi_{,a}\right) \\
&\quad - \tilde{\Gamma}^j\beta^i{}_{,j} + \frac{2}{3}\tilde{\Gamma}^i\beta^j{}_{,j} + \beta^k\tilde{\Gamma}^i{}_{,k} \\
&\quad + \tilde{\gamma}^{jk}\beta^i{}_{,jk} + \frac{1}{3}\tilde{\gamma}^{ij}\beta^k{}_{,kj} - 2\tilde{A}^{ia}\alpha_{,a} - (\chi_{yo} + \frac{2}{3})\left(\tilde{\Gamma}^i - \tilde{\gamma}^{kl}\tilde{\Gamma}^i_{kl}\right)\beta^m_{,m}
\end{aligned}
$$

where $d/dt = \partial/\partial t - \mathcal{L}_\beta$. The last term in $\tilde{\Gamma}^i$ equation suggested by Yo et al to suppress exponential growth of $\tilde{\Gamma}^i$ when $\beta^j{}_{,j} > 0$.

Initial Data

- Constraint equations are solved only at $t = 0$ to set up initial data.
- Assume conformal flatness and maximal slicing. ($\tilde{\gamma}_{ij} = \eta_{ij}, K = 0$)
- Take Bowen York form of extrinsic curvature

$$K^{ij} = \frac{3}{2r^2}(P^i n^j + P^j n^i - (\gamma^{ij} - n^i n^j)P^k n_k) + \frac{3}{r^3}(\epsilon^{ikl} S_k n_l n^j + \epsilon^{jkl} S_k n_l n^i)$$

- Puncture method: Let $\phi = \phi_{BL} + u$, $\phi_{BL} = 1 + \sum_{n=1}^{2} \frac{m_n}{2|\vec{r} - \vec{r_n}|}$ where the nth black hole has mass (parameter) m_n and is located at coordinate $\vec{r_n}$.

$$\Delta u + \beta(1 + \frac{u}{\phi_{BL}})^{-7} = 0, \beta = \frac{1}{8}\phi_{BL}^{-7} K^{ij} K_{ij}$$

- ϕ_{BL} is a solution that represents Einstein-Rosen bridge with the horizon located at the throat.

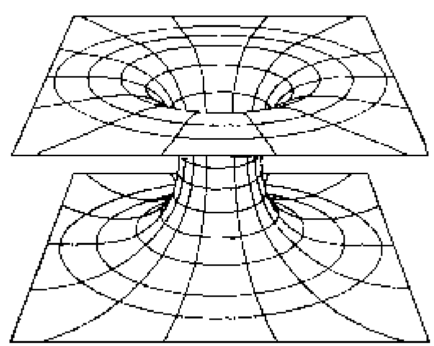

Gauge Conditions

- Gauge conditions do NOT change dynamics, but turn out to be crucial in getting stable numerical evolution.
- Gauge conditions: specify α, β^i. We currently use the following conditions (van Meter, Baker, Koppitz, Choi, PRD, 2006)

$$
\begin{aligned}
\partial_t \alpha &= -2\alpha K + \beta^i \partial_i \alpha \\
\partial_t \beta^i &= \frac{3}{4} B^i + \beta^j \partial_j \beta^i \\
\partial_t B^i &= \partial_t \tilde{\Gamma}^i - \beta^j \partial_j (\tilde{\Gamma}^j - B^i) - \eta B^i
\end{aligned}
$$

where η is a constant typically between $(1, 2)$.

Waveform Analysis

- Use Newman-Penrose Weyl tensor component Ψ_4 to analyse (outgoing) gravitational wave content.
- Harmonic decomposition

$$\Psi_4(r,\theta,\phi,t) = \sum_{lm} A_{lm}(r,t)_{-2}Y_{lm}(\theta,\phi)$$

$$A_{lm}(r,t) = \int \Psi_4(r,\theta,\phi,t)_{-2}Y_{lm}(\theta,\phi)d\Omega$$

- Given Ψ_4, one can calculate E, J_z, P_z.

$$\begin{aligned}
E &= \frac{r^2}{4\pi}\int\int_\Omega |\int_{-\infty}^t dt'\Psi_4(t',r,\theta,\phi)|^2 d\Omega dt \\
P_z &= \frac{r^2}{4\pi}\int\int_\Omega \cos\theta|\int_{-\infty}^t dt'\Psi_4(t',r,\theta,\phi)|^2 d\Omega dt \\
J_z &= -\frac{r^2}{4\pi}\int Re[\int_\Omega d\Omega(\partial_\phi \int_{-\infty}^t dt'\psi_4(t',r,\theta,\phi)) \\
&\times (\int dt' \int d\tilde{t}\bar{\psi}_4(\tilde{t},r,\theta,\phi))]dt
\end{aligned}$$

Some more details...

- Outer boundary conditions: We use simple out-going wave conditions for all variables at the edge of computational domain. But we usually try to “finish” the simulations within one light crossing time.
- Use 4th-order finite difference method for spatial derivatives to distretize Einstein equations on a “3D”-computational grid along with 4th-order Runge-Kutta time integrator.
- Adaptive mesh refinement, which is needed to properly handle a wide range of length scales in the problem, is a crucial component of our code. We follow an approach implemented in `PARAMESH`. Use `PARAMESH` package to implement parallelism and adaptivity.
- Scaling performance is good $\sim 86(67)\%$ level up to 1016(2032) CPUs for the full AMR simultaions (on Project Columbia, NASA Ames).

Computational grid structure

- Lapse function, α, on $z = 0$ slice: Size of the domain is $256M$, where M is initial total ADM mass-energy of the spacetime. Horizon size of the black holes $\sim M/2$.

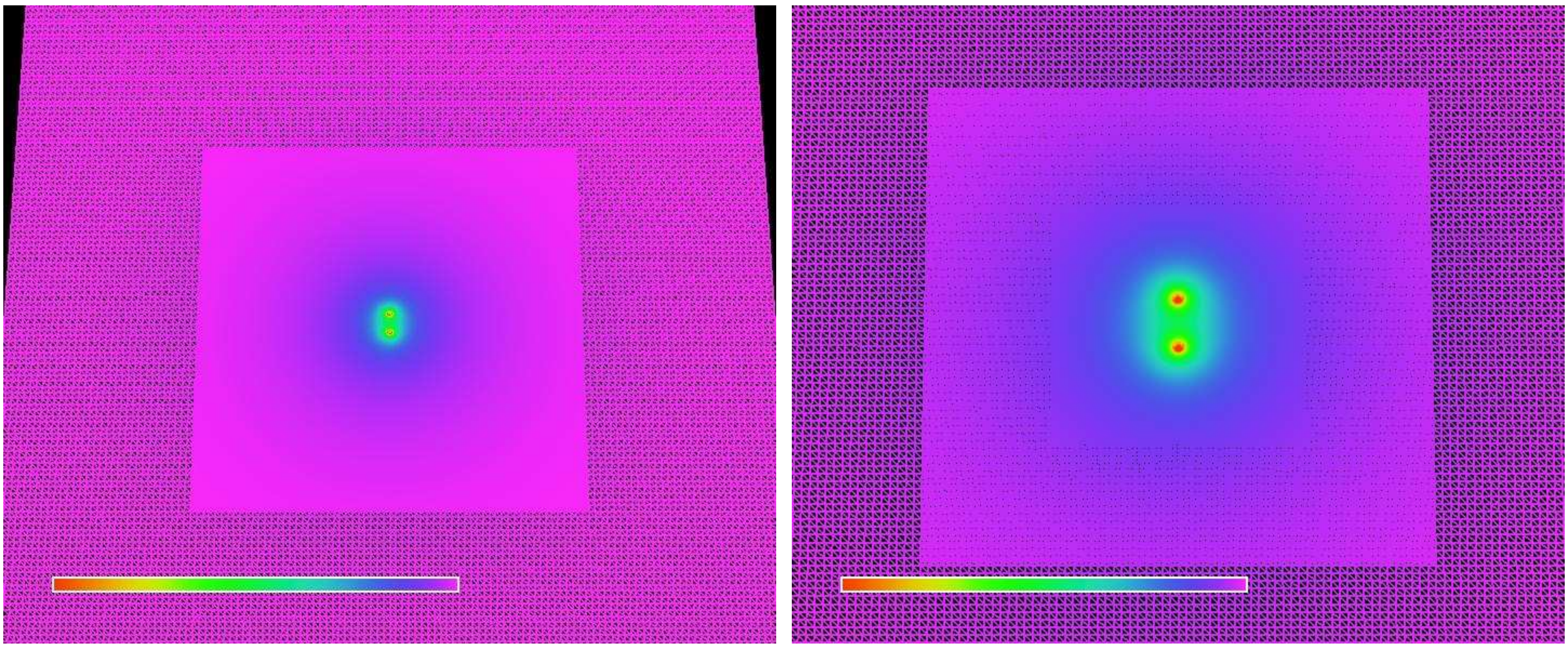

Computational grid structure

- Further zoom-in.
- Need fine resolutions around BHs. To resolve GWs, we can afford to use coarser resolution grids.

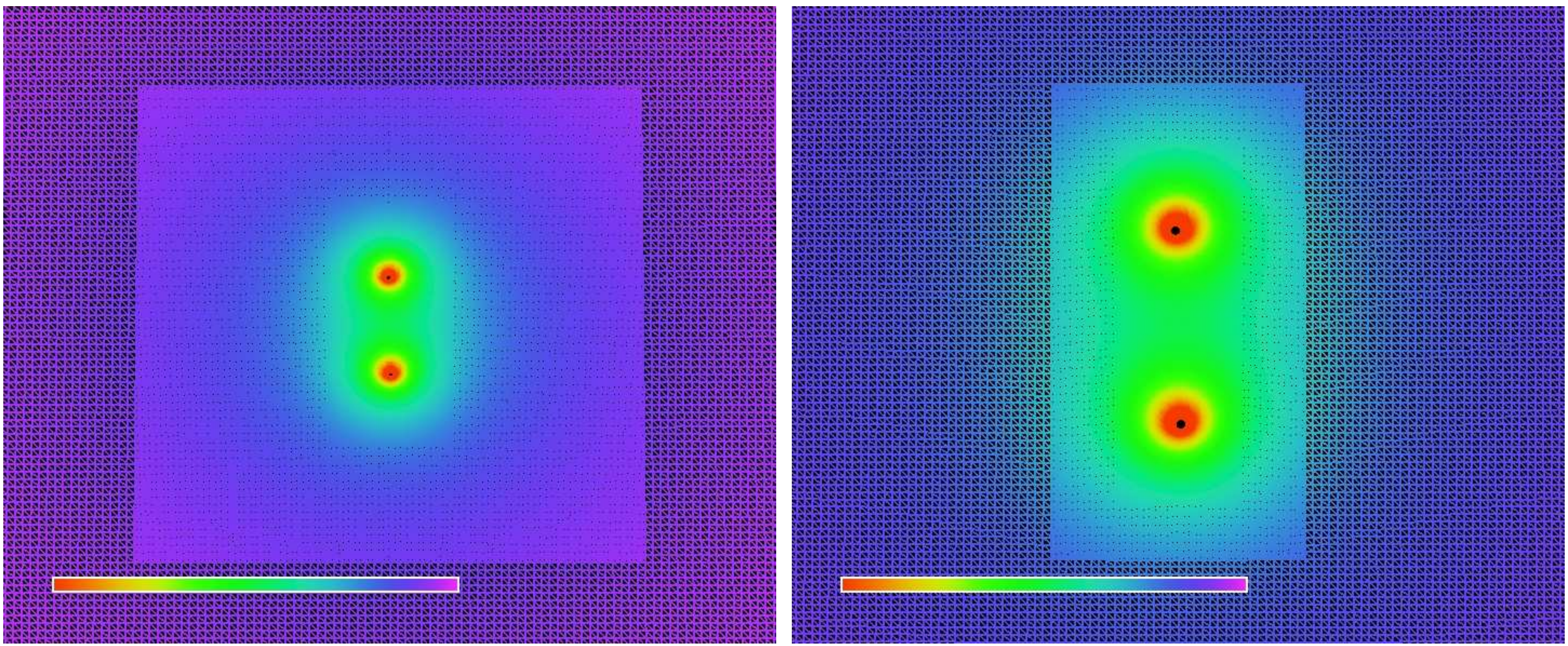

Computational grid structure

- Zoom-in around a single black hole: blackened regions indicate approximate locations of apparent horizons.
- During evolution, fine grids move along with moving black holes adaptively.

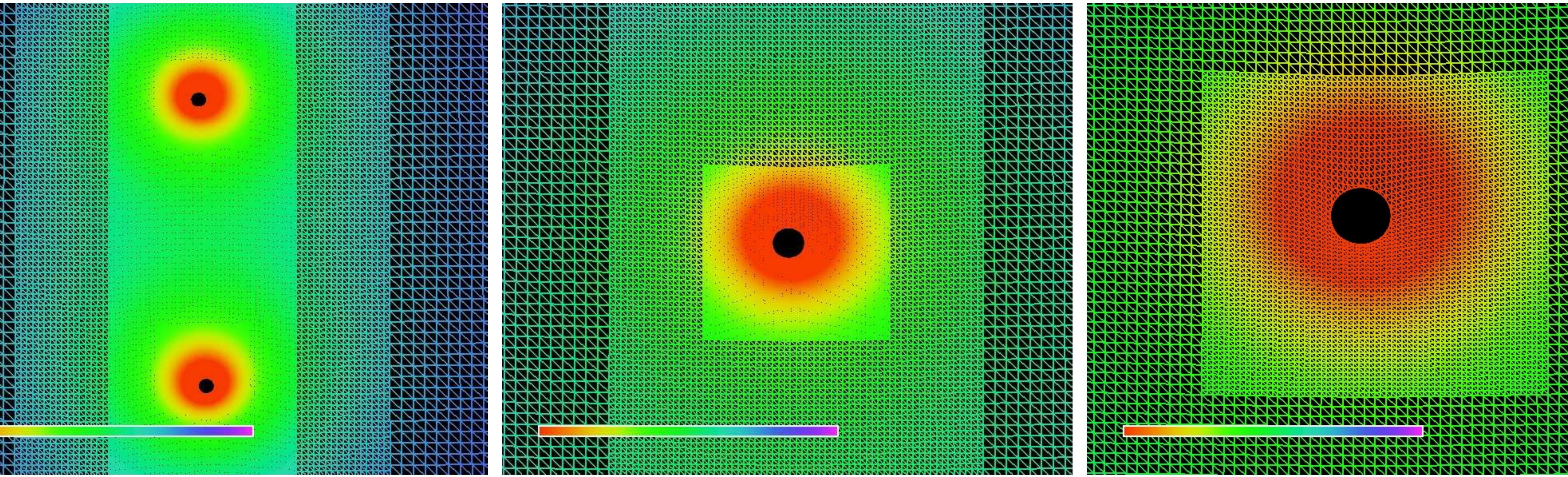

Results

- Equal mass & non-spinning quasi circular initial data.
  - Baker, Centrella, Choi, Koppitz, van Meter, Phys. Rev. Lett. **96**, 111102 (2006)
  - Baker, Centrella, Choi, Koppitz, van Meter, Phys. Rev. **D73**, 104002 (2006)
- Expect that astrophysically relevant binaries are in quasi-circular orbital configuration by the time they enter the phase where dynamics is dominated by gravitational wave emission.
- Main goals for these papers is to simulate the last few orbits of such situation. Here, we studied equal mass and non-spinning black hole binaries.
- Non-equal mass & non-spinning quasi circular initial data
  - Baker, Centrella, Choi, Koppitz, van Meter, Miller, in press, ApJ. Lett. astro-ph/0603204.
- Spinning black hole mergers
  - Choi, *et al*, in preparation (2006).

Equal mass & S=0 quasi-circular ID

- Binary is in quasi-circular orbit with initial separation between black holes along y-axis $\sim 9.9M$.
- $[MOVIE]$ of lapse function, α, on $z = 0$ plane
- Period of the first orbit $\sim 117M$; merges at $\sim 168M$.
- Note black excised regions indicate roughly where the apparent horizons are located.

Equal M & S=0: Grav. Waveforms

- Black hole binaries (initially equal mass and non-spinning black holes) lose about $3-4\%$ of the total energy, and $25-35\%$ of the total angular momentum through gravitational wave emission during the last two orbits, merger, and ringdown.
- For the merger of two $10^6 M_{sun}$ black holes, energy loss is about 10^{59} ergs.
- We ran a set of quasi-circular initial data with different initial separation. Found that the waveforms match well for the last orbit, merger, and ringdown.
- Ψ_4 is related to the strain amplitude, h: $\Psi_4 \sim \frac{\partial^2 h}{\partial t^2}$.
- $[MOVIE]$ isosurfaces of imaginary part of $L=2, M=2$ component of Ψ_4 from the simulation done with quasi-circular initial data with initial separation of $\sim 13.2M$.

Equal M & S=0: Grav. Waveforms

- Dominant component is $L = 2, M = 2$ harmonic mode.
- Plot of Re(rA_{22}) at a fixed r.

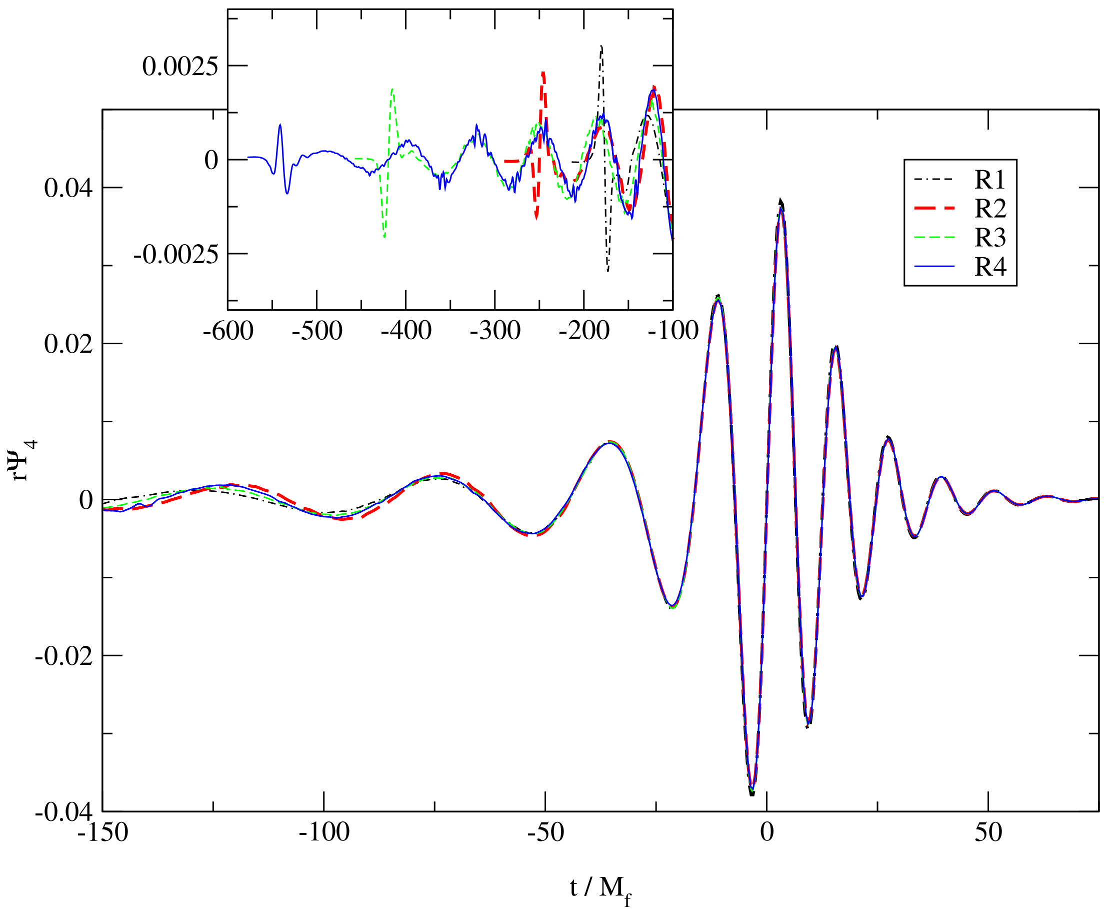

Non-equal mass & S=0 Initial Data

- Baker, Centrella, Choi, Koppitz, van Meter, Miller, in press, ApJ. Lett., astro-ph/0603204.
- Motivation: asymmetric emission of GWs can impart astrophysical kick to the merger remnant (seen from the center of mass observer).
- Large kick velocity comparable to escape velocity can unbound the merged black hole from the center of the host structure or kick the merged black hole completely out of the host structure $\rightarrow$ astrophysically very interesting and important value.
- Understanding of magnitude of kick velocities will have a major impact on astrophysics: Supermassive black hole evolution, structure formation.
- Calculations of GW-induced recoil kicks have a long history.
  - Recent Post-Newtonian results: Favata, Hughes, Holz (2004); Blanchet, Qusailah, Will (2005); Damour, Gopakumar (2006); Sopuerta, Yunes, Laguna (2006).
  - Recent numerical calculations by Goddard(2006), Campanelli (2005), PSU group (2006), U. of Jena group (2006).
- Calculations are difficult because we are trying to nail down small effects, $100 - 1000$km/s $\sim (0.01 - 0.001)c$.

Non-equal mass & S=0 initial data

- Mass ratio $\rho = M_1/M_2 = 2/3(= 0.667)$.
- $\Psi_4(t, x, y, z = 0)$ (real part) on $Z = 0$ plane

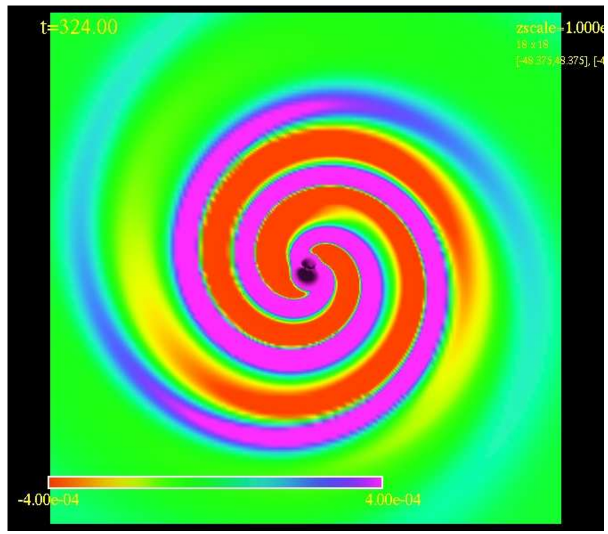

- Mode analysis indicate that dominant contribution comes from $L = 2, M = 2$ and $L = 3, M = 3$ mixing.
- Ψ_4 still dominated by $L = 2, M = 2$ mode and asymmetry is a very subtle effect.
- Our estimates for $\rho = 0.66$ is $86 - 97$km/s.

Recoil Velocity

- Waveforms at $r_{ext} = 30M$: $L = 2, M = 2$ part and $L = 3, M = 3$ part.

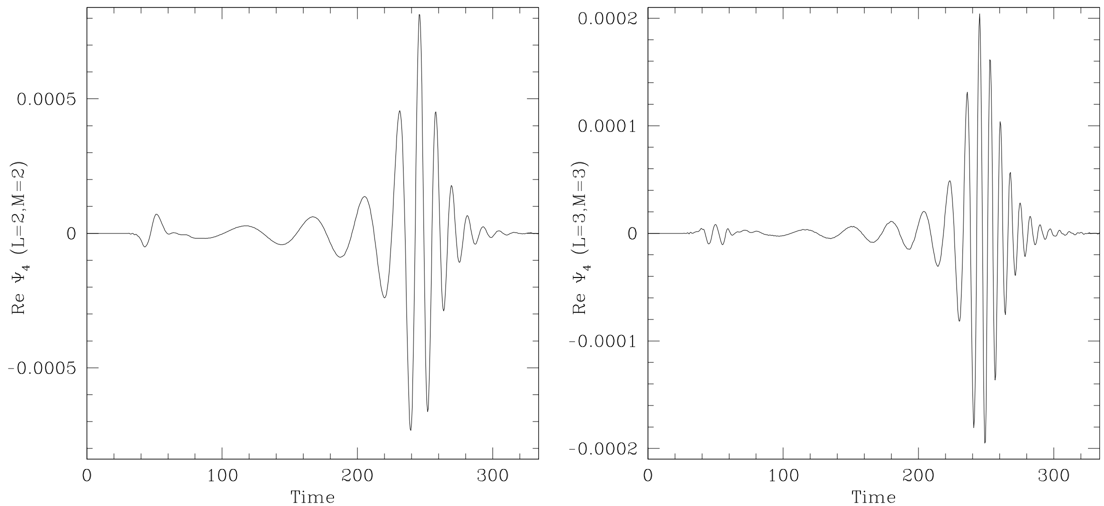

- $\omega_{22}/\omega_{33} \sim 2/3$.
- Simulations with three different initial separation (coord separation of $4.1M, 6.2M, 7.1M$) are used to analyze the final kick. ($h_f = M/32, M/40, M/48$)
- "kick" $= v(t) = \frac{1}{M}\sqrt{\left(\int^t \frac{dP_x(t')}{dt'}dt'\right)^2 + \left(\int^t \frac{dP_y(t')}{dt'}dt'\right)^2}$
- Kick velocity $\sim 92(\pm 5)$ km/s from the last orbit for $\rho = M_1/M_2 = 2/3$.

Spin Effects?

- There are indications that the supermassive black holes (as well as stellar mass black holes) are spinning fast although it is difficult to measure BH spins.
- We need to understand how important spin effects are (spin-orbit, spin-spin interactions, spin precessions, etc.) beyond Post-Newtonian limits.
- Early results in NR start to appear.
  - Campanelli, Lousto, Zlochower, PRD 74, 041501 (2006) & astro-ph/0608275.
  - They studied orbital hang-ups and spin-orbit interactions, but not kicks.
- I think there are at least two important areas:
  - Effects of spins on the recoil kick calculations.
  - Complexities in the waveforms?

Kicks from Spinning BHs: Preliminary

- Head-on collision between two spinning black holes. Initial spin vectors are perpendicular to the axis of collision (y-axis) and of equal magnitude but with opposite signs.

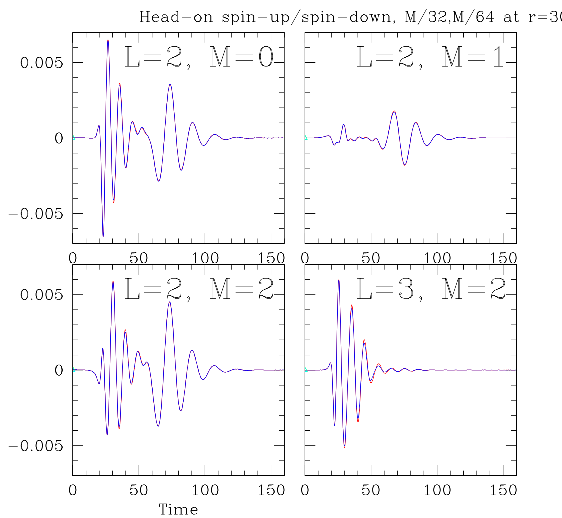

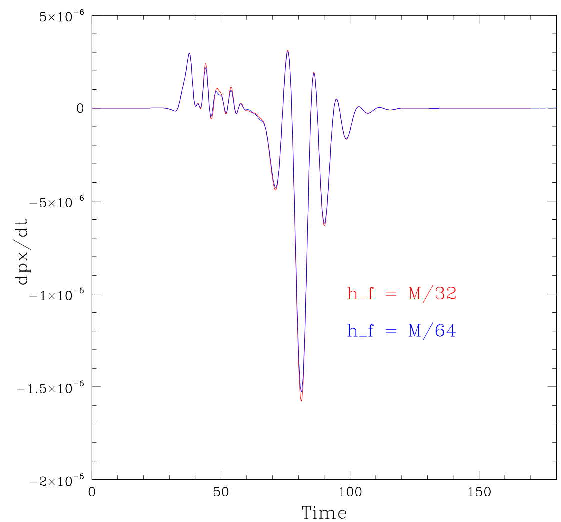

- Left (waveforms from simulations done with two different resolutions) Right ($\frac{dP_x}{dt}$ for two different resolutions). GWs are radiated mostly $-x$ directions, so the merged black holes are kicked to $+x$ directions.
- Estimated kick $\sim 33km/s$. This is significant amount for head-on collisions.
- Currently studying inspiral mergers of two spinning black holes with different masses.

Concluding Remarks

- Gravitational wave astrophysics will revolutionize our understanding of the universe as well as fundamental theories of gravitation.
- Numerical relativity is an indispensable tool in the studies of gravitation, especially in the strong and highly dynamical regimes.
- One of the key problems is study of the binary black hole mergers, understanding of dynamics and the resulting gravitational waveforms.
- Impact areas for BBH simulations
  - Detection & Parameter extraction.
  - Understanding & test of GR in the strong & dynamical regimes.
- Rapid progress and exciting results in the field over the last year or so. But still early stage in our understanding.
  - Mass ratio, spin.
  - More general scenarios.
  - Higher resolutions.

Concluding Remarks (con't)

- Access to large scale computing resources is crucial for success. We used up to 2000 CPUs at a time for our then-state-of-the-art simulations.
- Everyday exploratory simulations require ~ 100 or more CPUs on a regular basis.
- Numerical relativity is a good example of applications that will take full advantage of the next generation supercomputing environment (e.g. KISTI 4th generation supercomputer to be installed early 2007).
- PAYOFF IS HUGE: simulation results promise to have major impacts in various directions: gravitational wave data analysis, astrophysics, test of general relativity.